AD NUMBER

ADB204758

NEW LIMITATION CHANGE

TO

Approved for public release, distribution unlimited

FROM

Distribution authorized to DoD only. Other requests shall be referred to Embassy of Australia, Attn: Head Pub. Sec. Def/Sci., 1601 Massachusetts Ave., Washington, DC 20036.

AUTHORITY

DSTRO ltr, 18 May 2001.

DTIC

Input Impedance Calculation for TEM Horn Antennas

Geoff Staines and Sean Braidwood

DSTO

DEPARTMENT OF DEFENCE

DEFENCE SCIENCE AND TECHNOLOGY ORGANISATION

Input Impedance Calculation for TEM Horn Antennas

Geoff Staines and Sean Braidwood

Electronic Warfare Division
Electronics and Surveillance Research Laboratory

DSTO-TR-0187

ABSTRACT

This report describes a technique for calculating the input impedance of ideal, infinitely long TEM horn antennas used to radiate ultrawideband signals. A simple potential calculation is used to determine the fields of the TEM mode of the antenna, from which the input impedance is derived. This result is useful for matching TEM horns to the output impedance of the excitation source to avoid undesirable reflected signals.

DEPARTMENT OF DEFENCE

DEFENCE SCIENCE AND TECHNOLOGY ORGANISATION

Published by

DSTO Electronics and Surveillance Research Laboratory
PO Box 1500
Salisbury South Australia 5108

Telephone: (08) 259 5181
Fax: (08) 259 5938

AR-009-307
June 1995

Conditions of Release and Disposal

1. *This document is the property of the Australian Government; the information it contains is released for defence purposes only and must not be disseminated beyond the stated distribution without prior approval.*

2. *The document and information it contains must be handled in accordance with security regulations applying in the country of lodgement, downgrading instructions must be observed and delimitation is only with specific approval of the Releasing Authority as given in the Secondary Distribution statement.*

3. *This information may be subject to privately owned rights.*

4. *The officer in possession of this document is responsible for its safe custody. When no longer required this document should be destroyed and notification sent to: Senior Librarian, Defence Science and Technology Organisation Salisbury Research Library.*

Input Impedance Calculation for TEM Horn Antennas

EXECUTIVE SUMMARY

A simple numerical technique is described for calculating the input impedance of TEM horn antennas for ultrawideband (UWB) applications. UWB antennas are required to radiate subnanosecond pulses with minimal distortion. The required bandwidth is from a few hundred megahertz up to 10 gigahertz. TEM horn antennas have emerged as potential candidates for directional UWB applications such as impulse radar. The input impedance of the horn is typically matched to the output impedance of the source. At the DSTO Wideband Test Facility, the antenna geometry has previously been varied empirically to produce the required input impedance due to the unreliability of alternative theoretical techniques based on conformal mapping which was not corrected until recently. This simple analysis circumvents this time consuming process and is readily implemented.

Authors

Geoffrey W. Staines
Electronic Warfare Division

Geoff Staines received the BSc (Physics) degree from the University of Queensland in 1987, the BSc(Hons) from Flinders University in 1988, and a PhD in plasma physics from Flinders University in 1991. Since 1992, he has been a research scientist in Advanced Concepts Group, Electronic Warfare Division, DSTO Salisbury.

Sean Braidwood
Electronic Warfare Division

Sean Braidwood received the BSc.(Hons) from Adelaide University in 1989 and a MSc. in atomic physics from Flinders University in 1993. He is currently working for the Electronic Warfare Division, DSTO Salisbury.

Contents

1. Introduction

Recently there has been a growing interest in the possible defence applications of ultrawideband (UWB) radiation. These applications are currently being investigated at the DSTO Wideband Test Facility. The generation and transmission of these ultrawideband emissions such as impulse radiation, requires a fast electrical switch to generate a subnanosecond transient which directly excites a wideband antenna. If the excitation pulse, or more commonly its time derivative, is to be faithfully radiated in the far field zone, then a nondispersive antenna is required. This last requirement is a significant restriction, and rules out log-periodic antennas commonly used as compact, wideband antennas.

One class of antenna that is both wideband and nondispersive is the TEM horn, as shown in Figure 1.1. Two quasi-triangular plates are connected together at one vertex to form the feed. A spherical TEM wave propagates along the antenna structure, confined mainly between the plates. When the TEM mode reaches the end of the antenna structure, conversion to higher order propagating spherical TM and TE modes occurs because the TEM mode can no longer be supported. This type of antenna has been shown in the past to faithfully transmit the time derivative of the incident pulse in the far field zone [1].

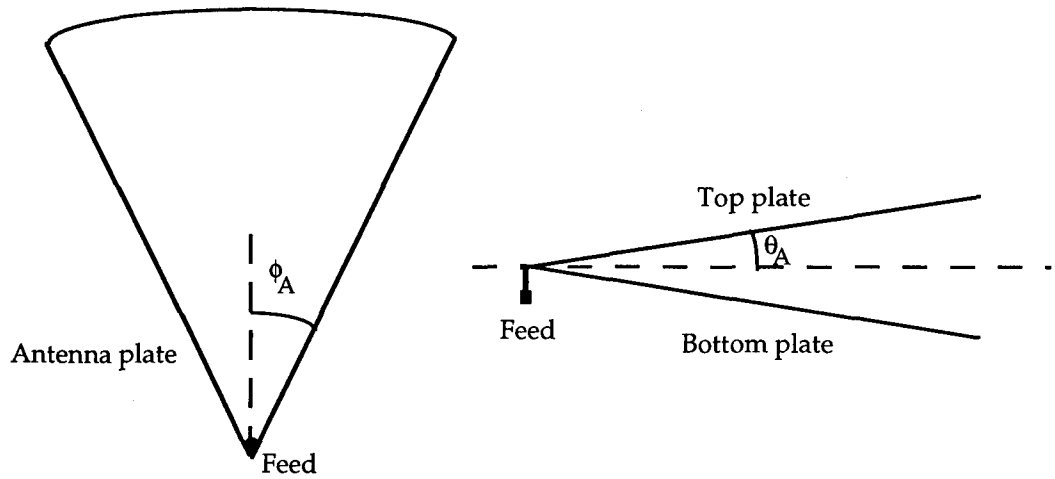

Figure 1.1: Conventional TEM horn geometry

The input impedance of TEM horns is dependent both on the flare angle θ_A and the apex angle of the plates, ϕ_A. For this analysis, the length of the horn is assumed to be much longer than the spatial width of the excitation pulse, so that reflections from the end of the horn can be ignored. For the 100 ps pulses normally used in the DSTO

Wideband Test Facility, the spatial pulse width is 3 cm. This is small compared to the TEM horn antenna plates which are usually 1 m long. Therefore, the input impedance of the horn is the same as for an ideal infinitely long antenna for frequencies of practical interest. Note that the impedance of an antenna which supports only the TEM mode is independent of frequency. The input impedance of the antenna is generally required to match that of the voltage source (typically 50 Ω). Previously, this match has been obtained empirically. This report describes a simple analysis based on a finite difference approach to calculate the TEM mode electric field of an ideal infinitely long horn. From the calculated field distribution for given angles θ_A and ϕ_A, the impedance is calculated from the power transmitted through the antenna.

Usually, ϕ_A is given and θ_A is to be found based on the desired antenna impedance. Note that as ϕ_A increases the beamwidth in the horizontal plane increases. To maintain the matching to the source impedance, θ_A must increase. This has the effect of decreasing the beamwidth in the vertical plane as ϕ_A increases. Antenna beamwidths are not predicted by this analysis, but the ability to calculate the value of θ_A required to match the antenna to the source impedance for a given ϕ_A removes one degree of freedom from the horn design. This considerably simplifies the design process.

Carrel [2] was the first to develop an analysis intended to calculate the input impedance of infinitely long TEM horn antennas. This technique relied upon conformal transformations to yield a simple analytic form for the impedance. Unfortunately, Carrel's analysis has been found to be incorrect due to an error in applying the conformal transformations. Lambert *et al* [3] have recently produced a revised version of Carrel's analysis which has been shown to yield the correct results. Note that until Lambert *et al* developed a corrected conformal mapping analysis, this technique was considered too unreliable to use. This report presents a simple two-dimensional analysis based on a finite-difference technique which does not require conformal mapping and is particularly simple to implement. In addition, antennas with arbitrary cross-sections in the (θ, ϕ) plane can be analysed since the technique is two-dimensional. This work arose from the application of a finite-difference time-domain analysis for ultrawideband antenna modelling [4]. The results of this finite-difference technique are in good agreement with experimentally measured input impedance values for several TEM horns.

2. Theory

2.1 The Finite Difference Calculation

From Collin [5], a TEM mode electric field in spherical geometry can be related to scalar functions g and Φ by

$$\mathbf{E} = g(r)\nabla_t\Phi$$

where $\Phi(\theta,\phi)$ satisfies

$$\nabla_t^2\Phi = 0$$

and $g(r)$ follows

$$\frac{d^2g}{dr^2} + k^2 g(r) = 0$$

with $k = \omega\sqrt{\mu_0\varepsilon_0}$. Therefore

$$g(r) = e^{-jkr}$$

and

$$\left[\sin^2\theta\frac{\partial^2}{\partial\theta^2} + \sin\theta\cos\theta\frac{\partial}{\partial\theta} + \frac{\partial^2}{\partial\phi^2}\right]\Phi(\theta,\phi) = 0 \qquad (1)$$

Note that Equation 1 does not contain any dependence on k and hence frequency. Therefore, this analysis applies directly in either the frequency or time domain. The potential $\Phi(\theta,\phi)$ can be represented as $\Phi(i,j)$ on a spherical finite difference mesh discretised in θ and ϕ using

$$\theta_i = \frac{\pi}{2} - i\,\Delta_\theta \quad \text{and} \quad \phi_j = \frac{\pi}{2} + j\,\Delta_\phi$$

where

$$\Delta_\theta = \frac{\pi}{2(N_\theta+1)} \quad \text{and} \quad \Delta_\phi = \frac{\pi}{N_\phi}$$

for $i = 0, 1,..., N_\theta$, and $j = 0, 1,..., N_\phi$. Symmetry allows the entire antenna to be analysed by considering only the quadrant $\theta = 0$ to $\pi/2$ and $\phi = \pi/2$ to $3\pi/2$. The spherical coordinate system is shown in Figure 2.1.

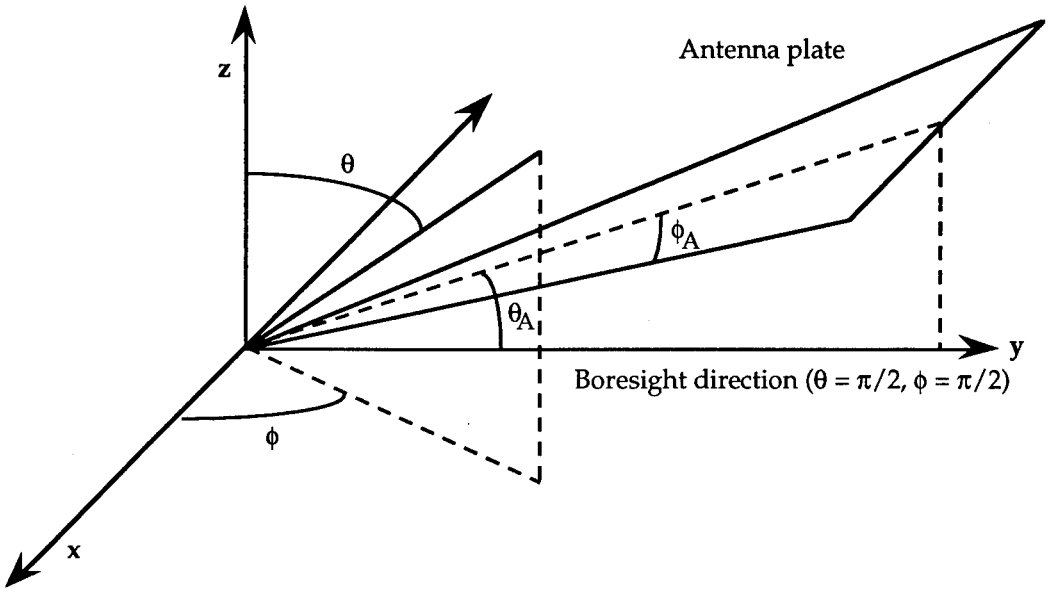

Figure 2.1: Coordinate system for TEM horn input impedance analysis

The antenna plate was assumed to have zero thickness and extend over ϕ from $j = 0$ to $j = j_{plate}$ at the theta value corresponding to $i = i_{plate}$. This requirement for discretisation for the finite difference representation of Equation 1 meant that the flare and apex plate angles of the antenna, θ_A and ϕ_A, were rounded off to the nearest (θ_i,ϕ_j) values on the mesh. The effect of this rounding could be minimised by a judicious choice of N_θ and N_ϕ.

Expressing Equation 1 in its finite difference form leads to

$$\Phi(i+1,j)\frac{\sin\theta}{\Delta_\theta}\left[\frac{\sin\theta}{\Delta_\theta}+\frac{\cos\theta}{2}\right]+\Phi((i-1,j)\frac{\sin\theta}{\Delta_\theta}\left[\frac{\sin\theta}{\Delta_\theta}-\frac{\cos\theta}{2}\right]-2\,\Phi(i,j)\left[\frac{\sin^2\theta}{\Delta_\theta^2}+\frac{1}{\Delta_\phi^2}\right]$$

$$+\Phi(i,j+1)\frac{1}{\Delta_\phi^2}+\Phi(i,j-1)\frac{1}{\Delta_\phi^2} \;=\; 0 \qquad (2)$$

This can be written as

$$\mathbf{A}\,\Phi \;=\; \mathbf{b} \qquad (3)$$

where

$$\Phi_k \;=\; \Phi(i,j)$$

$$\mathbf{A}_{kk} = -2\left[\frac{\sin^2\theta}{\Delta_\theta^2} + \frac{1}{\Delta_\phi^2}\right]$$

$$\mathbf{A}_{k(k-1)} = \mathbf{A}_{k(k+1)} = \frac{1}{\Delta_\phi^2}$$

$$\mathbf{A}_{k(k+jmax)} = \frac{\sin\theta}{\Delta_\theta}\left[\frac{\sin\theta}{\Delta_\theta} + \frac{\cos\theta}{2}\right]$$

$$\mathbf{A}_{k(k-jmax)} = \frac{\sin\theta}{\Delta_\theta}\left[\frac{\sin\theta}{\Delta_\theta} - \frac{\cos\theta}{2}\right]$$

otherwise

$$\mathbf{A}_{kl} = 0$$

for $k = i\,(N_\phi+1) + j$. For free space, $\mathbf{b}_k = 0$ for all k, however $\mathbf{A}_{kl}$ and $\mathbf{b}_k$ will also include the boundary conditions which are described in the next section.

Equation 3 can be solved using successive overrelaxation based on a Gauss-Seidel iterative algorithm. An initial estimate of the potential $\Phi(i,j)$ is made for all i, j. The value for the potential at each grid point is updated using

$$\Phi_k^{(m+1)} = (1-\omega)\,\Phi_k^{(m+1)} - \omega\,\frac{\sum_{l<k} \mathbf{A}_{kl}\,\Phi_k^{(m)} + \sum_{l>k} \mathbf{A}_{kl}\,\Phi_k^{(m)} - \mathbf{b}_k}{\mathbf{A}_{kk}}$$

The iteration was halted when the average magnitude of the correction to the potential over the entire mesh was less than 10^{-5} typically. This condition was used to specify adequate convergence.

The relaxation parameter ω is given by

$$\omega = \frac{2}{1+\sqrt{1-\mu^2}}$$

where μ is the spectral radius of the block Jacobi matrix $\mathbf{B} = -\mathbf{D}^{-1}(\mathbf{L}+\mathbf{U})$ corresponding to $\mathbf{A} = \mathbf{D} + \mathbf{L} + \mathbf{U}$ [6]. **D**, **L**, and **U** are the diagonal, upper triangular, and lower triangular elements of **A**, respectively. The spectral radius μ is the largest eigenvalue of **B**, which can be readily calculated [7].

Once calculated, the potential can be used to determine the electric and therefore the magnetic field of the TEM mode in the antenna.

2.2 Boundary Conditions

Boundary conditions were required at the edges of the mesh. For $\theta = 0$ ($i = 0$), the potential Φ was zero, since the antenna was represented by a positively charged plate at $\theta = +\theta_A$ and a negatively charged plate at $\theta = -\theta_A$. Therefore when $i = 0$,

$$\mathbf{A}_{kk} = 1 \text{ and } \mathbf{A}_{k(k-1)} = \mathbf{A}_{k(k-1)} = \mathbf{A}_{k(k-j_{max})} = \mathbf{A}_{k(k+j_{max})} = 0$$

At $\theta = \theta_A$ ($i = i_{plate}$), the potential was set to $V_0/2$, where V_0 is the total potential difference across the plates. Therefore for $i = i_{plate}$,

$$\mathbf{A}_{kk} = 1 \text{ and } \mathbf{A}_{k(k-1)} = \mathbf{A}_{k(k-1)} = \mathbf{A}_{k(k-j_{max})} = \mathbf{A}_{k(k+j_{max})} = 0$$

and

$$\mathbf{b}_k = V_0/2$$

Since the TEM horn antenna is symmetric about the y-z plane in figure 2.1,

$$\frac{\partial \Phi}{\partial \phi} = 0 \text{ at } \phi = \frac{\pi}{2} (j = 0) \text{ and } \phi = \frac{3\pi}{2} (j = N_\phi)$$

Hence $\Phi(i,j\text{-}1) = \phi(i,j\text{+}1)$, which means that for $j = 0$

$$\mathbf{A}_{k(k+1)} = \frac{1}{\Delta_\phi^2}$$

and for $j = N_\phi$

$$\mathbf{A}_{k(k-1)} = \frac{1}{\Delta_\phi^2}$$

The final boundary condition was derived for the potential $\theta = 0$ position at the top of the spherical mesh. At this point, the potential $\Phi = \Phi_{top}$. As $\theta \rightarrow 0$, Equation 1 infers that

$$\frac{\partial^2 \Phi}{\partial \phi^2} \rightarrow 0$$

If the potential in the vicinity of $\theta = 0$ ($i = N_\theta$) is represented in terms of ϕ harmonics as

$$\Phi = \sum_{n=0}^{\infty} \Phi_n e^{jn\phi}$$

then

$$-n^2 \Phi_n \rightarrow 0$$

This implies that $\Phi_n = 0$ near $\theta = 0$ for $n \neq 0$. The $n = 0$ component can be found by averaging the nearest neighbour values. From continuity of the electric field in free space, the $n = 0$ component of Φ at $\theta = 0$ can be approximated by the value at $\theta = \Delta_\theta$, since

$$\frac{d\Phi_0}{d\theta} \rightarrow 0 \quad \text{as} \quad \theta \rightarrow 0.$$

Therefore, for $\theta = \Delta_\theta$ ($i = N_\theta$) Equation 2 can be written as

$$\Phi(N_\theta\text{-}1,j) \frac{\sin\theta}{\Delta_\theta}\left[\frac{\sin\theta}{\Delta_\theta} - \frac{\cos\theta}{2}\right] - 2\,\Phi(N_\theta,j)\left[\frac{\sin^2\theta}{\Delta_\theta^2} + \frac{1}{\Delta_\phi^2}\right] + \Phi(N_\theta,j+1)\frac{1}{\Delta_\phi^2} + \Phi(N_\theta,j\text{-}1)\frac{1}{\Delta_\phi^2}$$

$$= -\Phi_{top} \frac{\sin\theta}{\Delta_\theta}\left[\frac{\sin\theta}{\Delta_\theta} + \frac{\cos\theta}{2}\right]$$

where

$$\Phi_{top} = \frac{1}{N_\phi+1} \sum_{j=0}^{N_\phi} \Phi(N_\theta,j)$$

Therefore, no modifications to $\mathbf{A}_{kl}$ need be made, and $\mathbf{b}_k$ is now given by

$$\mathbf{b}_k = -\frac{\sin\theta}{\Delta_\theta}\left[\frac{\sin\theta}{\Delta_\theta} + \frac{\cos\theta}{2}\right]\frac{1}{N_\phi+1} \sum_{j=0}^{N_\phi} \Phi(N_\theta,j)$$

for $i = N_\theta$.

2.3 Electric Field Calculation

The electric field quantities $\alpha_\theta(i,j)$ and $\alpha_\phi(i,j)$ which are related to the electric field through

$$E_\theta = V_0 \frac{\alpha_\theta(i,j)}{r} \quad \text{and} \quad E_\phi = V_0 \frac{\alpha_\phi(i,j)}{r}$$

are calculated in the centre of the finite difference mesh cells using the values of the potential at the vertices of the cells as follows

$$\alpha_\theta(i,j) = -\frac{\partial \Phi}{\partial \theta} = \frac{\Phi(i,j+1) + \Phi(i,j) - \Phi(i+1,j) - \Phi(i+1,j+1)}{2\,\Delta_\theta}$$

$$\alpha_\phi(i,j) = -\frac{1}{\sin\theta}\frac{\partial \Phi}{\partial \phi} = \frac{\Phi(i,j) + \Phi(i+1,j) - \Phi(i,j+1) - \Phi(i+1,j+1)}{2 \sin\theta\,\Delta_\phi}$$

$\alpha_\theta(\theta,\phi)$ and $\alpha_\phi(\theta,\phi)$) can be found for the other three quadrants using

$$\alpha_\phi(\theta_i,\phi_j) = -\alpha_\phi(-\theta_i,\phi_j) = -\alpha_\phi(\theta_i,-\phi_j) = \alpha_\phi(-\theta_i,-\phi_j)$$

and

$$\alpha_\theta(\theta_i,\phi_j) = \alpha_\theta(-\theta_i,\phi_j) = \alpha_\theta(\theta_i,-\phi_j) = \alpha_\theta(-\theta_i,-\phi_j)$$

The electric field can now be calculated for the TEM mode of the antenna from the potential calculated on the finite difference mesh. The input impedance can now be calculated from the TEM mode field.

2.4 Input Impedance Calculation

The input impedance was determined by calculating the power, P, transmitted through a spherical surface enclosing the antenna as follows

$$P = \int_0^{\pi} \int_0^{2\pi} \frac{|\mathbf{E}|^2}{\zeta_0} a^2 \sin\theta \, d\phi \, d\theta$$

where $|\mathbf{E}|$ is the magnitude of the electric field, ζ_0 is the impedance of free space, and a is the radius of the spherical surface. Using symmetry and substituting for the electric field, P can be expressed as

$$P = 4\frac{V_0^2}{\zeta_0} \int_0^{\pi/2} \int_{\pi/2}^{3\pi/2} (\alpha_\theta^2 + \alpha_\phi^2) \sin\theta \, d\phi \, d\theta$$

The power can also be related to the voltage across the plates, V_0, and the antenna input impedance, Z_A, using

$$P = \frac{V_0^2}{Z_A}$$

Therefore

$$Z_A = \frac{\zeta_0}{4 \int_0^{\pi/2} \int_{\pi/2}^{3\pi/2} (\alpha_\theta^2 + \alpha_\phi^2) \sin\theta \, d\phi \, d\theta}$$

In most practical situations, the TEM horn will be fed by 50 Ω coax with an applied voltage V_{in}. If the antenna is matched to the feed cable, then $V_0 = V_{in}$. However, when there is a mismatch, the voltage on the antenna plates is related to the applied voltage by

$$V_0 = \frac{2 Z_A}{Z_A + Z_{coax}} V_{in}$$

where $Z_{coax} = 50\ \Omega$.

The finite difference potential calculation therefore allows the input impedance of the TEM horn to be calculated from the TEM mode fields and from power considerations. The only approximations are due to the finite difference mesh discretisation and the small rounding of the antenna flare and apex angles, θ_A and ϕ_A, as described in Section 2.1.

3. Results

The antenna input impedance was measured for plate apex angles of 20°, 30°, and 45° using a single triangular fin supported above a ground plane, with the antenna fed from underneath the ground plane via an N-type connector. The impedance of this configuration is half the impedance of a full horn. The impedance was determined for a range of flare angles, θ_A from the reflection coefficient. The flare angle was limited to 30° due to mechanical constraints on the feed. Reflections from the aperture of the antenna were time-gated out so that the measurements could be related to infinitely long antennas. A Hewlett-Packard HP54120A 18 GHz digitising oscilloscope was used with an HP 54121A four-channel test set which possessed a time-domain reflectometry (TDR) capability. The reflection coefficient, ρ, for each antenna configuration was determined by measuring the amplitude of the reflected voltage, E_r, and dividing it by the height of the incident voltage step E_i, which was measured as 200 mV.

$$\rho = \frac{E_r}{E_i}$$

The error in ρ was calculated from the error in E_r and E_i, $\sigma(E)$, using

$$\sigma(\rho) = \frac{\sqrt{1+\rho^2}}{E_i}\sigma(E)$$

The error $\sigma(E)$ was set to the cursor width of ±1.56 mV.

The antenna input impedance was calculated from the reflection coefficient using

$$Z_A = Z_0 \frac{1-\rho}{1+\rho}$$

where $Z_0 = 50\ \Omega$ is the impedance of the oscilloscope input. The impedance error $\sigma(Z_A)$ was calculated from the error in the reflection coefficient

$$\sigma(Z_A) = \frac{2\,Z_A}{(1-\rho)^2}\sigma(\rho)$$

Table 3.1 shows the measured input impedance Z_A^{exp} and the error, $\sigma(Z_A^{exp})$ together with the theoretical results Z_A^{th} from the finite difference potential calculation, for various flare angles, θ_A, for the 20° apex angle TEM horn. Tables 3.2 and 3.3 show the same parameters for 30° and 45° apex angle horns. These results are plotted in Figures 3.1, 3.2, and 3.3. The theoretical results are the continuous curves and the points correspond to measured impedance values. The agreement between the theoretical and experimental results is usually within experimental error. The calculated impedance was found to be systematically greater than the measured impedance for the 45° apex angle horn, as shown in Table 3.3 and Figure 3.3. This was probably due to the mechanical difficulties involved in rigidly supporting the large triangular plate above the ground plane.

The number of finite difference mesh points, N_θ and N_ϕ, were typically in the range 100-150. The tolerance for the overrelaxation scheme was 10^{-5}. Under these conditions, the run time on a Sun SPARC 5 workstation was approximately 2-5 minutes for each flare and apex angle.

Table 3.1: Measured and theoretical TEM horn input impedances for 20° apex angle

θ_A (deg)	$Z_A^{exp}(\Omega)$	$\sigma(Z_A^{exp})$ (Ω)	Z_A^{th} (Ω)
5.739	76.6	1.2	75.4
6.892	85.5	1.4	86.9
8.048	96.9	1.5	94.6
9.207	104.8	1.6	106.1
10.37	113.3	1.8	114.9
11.54	122.6	1.9	123.3
12.71	128.6	2.1	131.4
13.89	137.0	2.2	136.13
15.07	144.6	2.4	143.8
16.26	151.0	2.5	151.0
17.46	156.0	2.6	157.1
18.66	161.2	2.7	162.3
19.88	169.5	2.9	166.3
21.10	172.3	3.0	171.9
22.33	178.3	3.1	177.1
23.58	184.4	3.3	182.1
24.83	187.6	3.4	186.5
26.10	194.2	3.5	189.5
27.39	197.7	3.6	193.6
28.69	201.2	3.7	197.5
30	204.8	3.8	201.4

Table 3.2: Measured and theoretical TEM horn input impedances for 30° apex angle

θ_A (deg)	$Z_A^{exp}(\Omega)$	$\sigma(Z_A^{exp})$ (Ω)	Z_A^{th} (Ω)
6.6	59.0	1.0	62.7
8.0	68.4	1.1	72.1
9.3	77.8	1.2	80.7
10.7	85.5	1.4	86.6
12.0	92.5	1.5	94.5
13.4	100.0	1.6	101.7
14.8	106.5	1.7	108.5
16.1	113.3	1.8	114.9
17.5	118.8	1.9	120.8
18.9	124.6	2.0	126.3
20.3	130.6	2.1	131.6
21.7	137.0	2.2	136.4
23.2	141.5	2.3	141.0
24.6	146.1	2.4	145.4
26.1	151.0	2.5	149.4
27.6	156.0	2.6	153.3
29.1	158.6	2.7	156.9
30.6	163.9	2.8	161.3
32.2	166.7	2.9	164.3

Table 3.3: Measured and theoretical TEM horn input impedances for 45° apex angle

θ_A (deg)	Z_A^{exp} (Ω)	$\sigma(Z_A^{exp})$ (Ω)	Z_A^{th} (Ω)
5.7	35.5	0.8	38.7
6.9	40.7	0.8	45.6
8.0	46.3	0.9	50.5
9.2	51.5	0.9	56.2
10.4	57.1	1.00	62.7
11.5	61.0	1.04	67.6
12.7	66.2	1.1	72.5
13.9	71.8	1.2	76.8
15.0	76.6	1.2	81.2
16.3	80.3	1.3	85.6
17.5	84.2	1.3	89.8
18.7	88.2	1.4	93.9
19.9	92.5	1.5	97.3
21.1	96.9	1.5	101.0
22.3	100.0	1.6	104.5
23.6	103.2	1.6	107.7
24.8	108.1	1.7	110.8
26.1	111.6	1.8	114.1
27.4	115.1	1.8	116.8
28.7	117.0	1.8	119.8
30	120.7	1.9	122.6

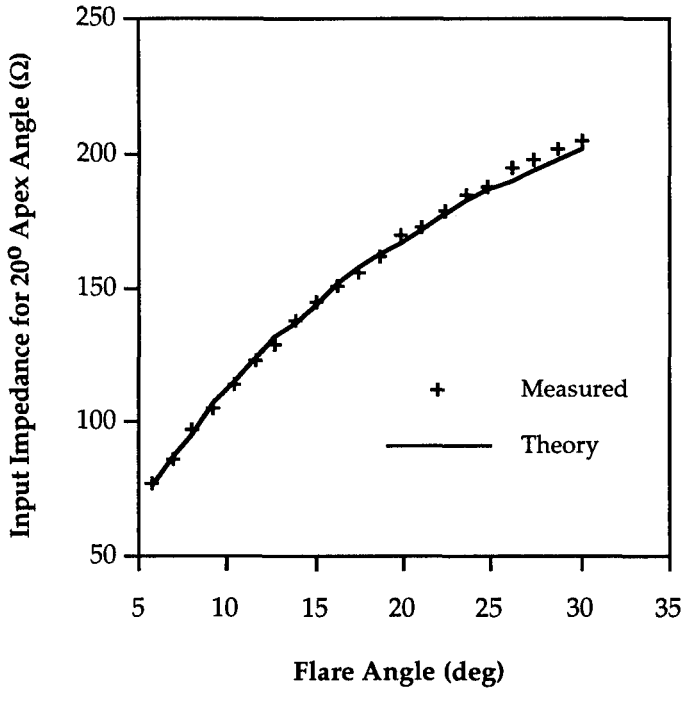

Figure 3.1: Input impedance against flare angle θ_A for TEM horn with 20° apex angle

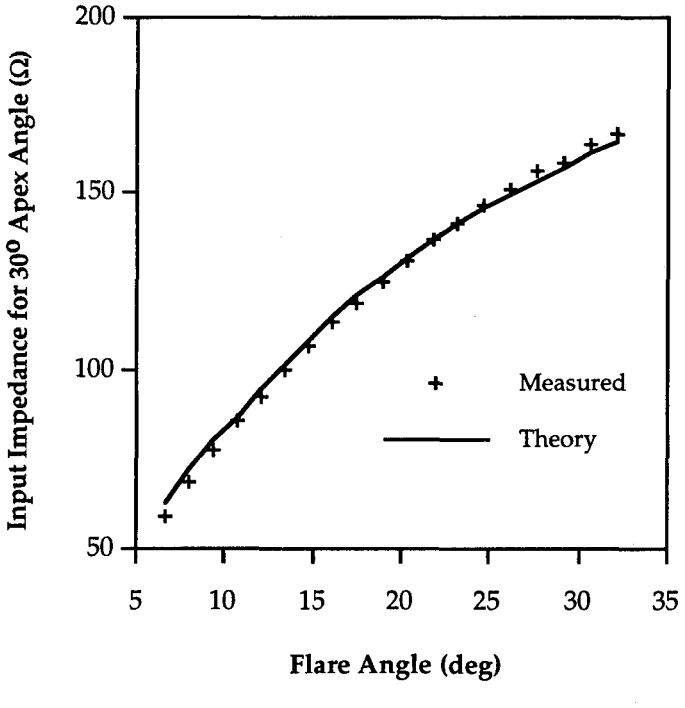

Figure 3.2: Input impedance against flare angle θ_A for TEM horn with 30° apex angle

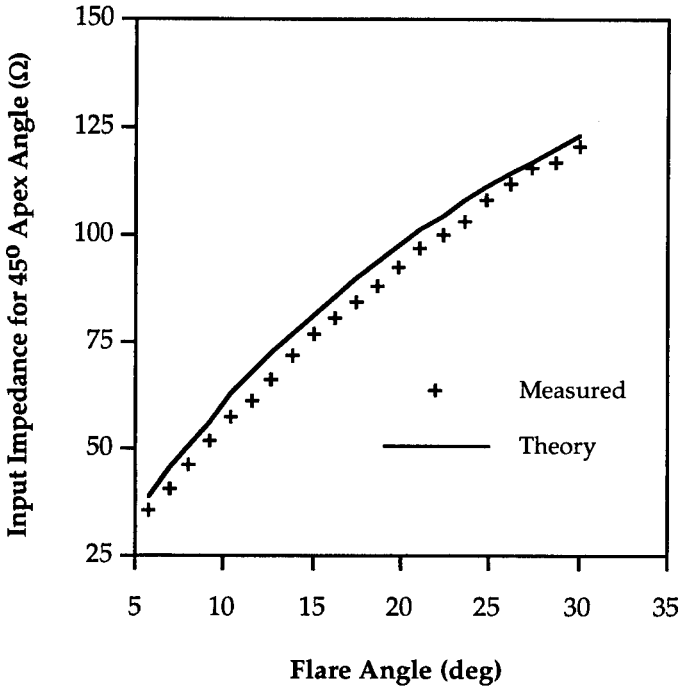

Figure 3.3: Input impedance against flare angle θ_A for TEM horn with 45° apex angle

4. Conclusions

A relatively simple analysis has been presented which is useful for calculating the input impedance of TEM horn antennas suitable for radiating ultrawideband pulses. For ideal, infinitely-long antennas the input impedance is independent of frequency. This approximation is valid provided the length of the horn is much greater than the spatial pulse width. This is certainly the case for the TEM horns used in the DSTO Wideband Test Facility which are usually 1 m in length. A finite difference calculation in spherical geometry was used to calculate the TEM mode potential which could then be used to calculate the input impedance of the antenna with considerable accuracy. This approach is simpler than alternative conformal mapping techniques [2], [3] which until recently have been considered as unreliable. Experimental data agrees well with the theoretical predictions for the TEM horn input impedance. For plate apex angles of 20° and 30°, the agreement between the measured and predicted impedance values is generally better than a few percent. The discrepancy between theoretical and experimental results was somwhat worse for the horn with a 45° apex angle at approximately 10%. This was attributed to mechanical difficulties in supporting the plate. This analysis can now be used to simplify the

design of TEM horn antennas by allowing θ_A to be calculated for a given ϕ_A and excitation source output impedance.

5. References

[1] D.M. Parkes, P.D. Smith, "Practical method of predicting transient fields and monopole current waveforms," *IEE Proceedings*, Vol. 135, Pt. H, No. 4, August 1988, pp. 231-236.

[2] R.L. Carrel, "The characteristic impedance of two infinite cones of arbitrary cross-section," *IEEE Transactions on Antennas and Propagation*, Vol. 6, April 1958, pp. 197-201.

[3] A.P. Lambert, S.M. Booker, P.D. Smith, "Calculation of the characteristic impedance of TEM horn antennas using the conformal mapping approach," *IEEE Transactions on Antennas and Propagation*, Vol. 43, No. 1, Jan 1995, pp. 47-53.

[4] G. Staines, S. Braidwood, "A finite-difference time-domain analysis for rotationally symmetric ultrawideband antennas," *DSTO Research Report DSTO-RR-0019*, Feb. 1995.

[5] R.E. Collin, *Field Theory of Guided Waves, Second Edition*, IEEE Press, 1991, p. 174.

[6] D. Potter, *Computational Physics*, John Wiley and Sons, 1973, ISBN 0 471 69555 6, p. 108.

[7] *ibid*, p. 114.

Input Impedance Calculation for
TEM Horn Antennas

Geoff Staines and Sean Braidwood

(DSTO-TR-0187)

DISTRIBUTION

	Number of Copies.
DEPARTMENT OF DEFENCE	
Defence Science and Technology Organisation	
Chief Defence Scientist and members of the	) 1 shared copy
DSTO Central Office Executive	) for circulation
Counsellor Defence Science, London	Doc Control Data Sheet Only
Counsellor Defence Science, Washington	Doc Control Data Sheet Only
Scientific Adviser POLCOM	1
Senior Defence Scientific Adviser	1
Assistant Secretary Scientific Analysis	1
Director, Aeronautical and Maritime Research Laboratory	1
Electronics and Surveillance Research Laboratory	
Chief, Electronic Warfare Division	1
Research Leader, Electronic Countermeasures	1
Head, Advanced Concepts Group	1
Dr Bevan.D. Bates	1
Dr Geoffrey W. Staines	1
Mr Sean W. Braidwood	1
Navy Office	
Navy Scientific Adviser	1
Army Office	
Scientific Adviser - Army	1
Air Office	
Air Force Scientific Adviser	1
Defence Intelligence Organisation	
Director, Scientific Analysis Branch. Att. Head, Electronics	1
HQADF	
Director, Directorate of Communications Engineering	1
Director General, Force Development (Sea)	1
Director General, Force Development (Air)	1

Director General, Force Development (Land)	1
Director General, Force Development (Joint)	1
Libraries and Information Services	
Defence Central Library, Technical Reports Centre	1
Manager, Document Exchange Centre (for retention)	1
National Technical Information Services, United States	2
Defence Research Information Centre, United Kingdom	2
Defence Science and Technology Organisation Salisbury, Research Library	2
Library Defence Signals Directorate, Canberra	1
Spares, DSTOS, Research Library	6

Department of Defence

DOCUMENT CONTROL DATA SHEET

1. Page Classification	
UNCLASSIFIED	
2. Privacy Marking/Caveat	

3a. AR Number	3b. Establishment Number	3c. Type of Report	4. Task Number	
AR-009-307	DSTO-TR-0187	TECHNICAL REPORT	ADF 93/284	
5. Document Date	6. Cost Code	7. Security Classification	8. No. of Pages	26
JUNE 1995	839262	[L] [U] [U]	9. No. of Refs.	7

10. Title
INPUT IMPEDANCE CALCULATION FOR TEM HORN ANTENNAS

Document Title Abstract
S (Secret C (Confi) R (Rest) U (Unclass)

* For UNCLASSIFIED docs with a secondary distribution LIMITATION, use (L) in document box.

11. Author(s)
Geoff Staines
Sean Braidwood

12. Downgrading/ Delimiting Instructions
Limitation to be reviewed in March 2000

13a. Corporate Author and Address
Electronic Warfare Division
Electronics and Surveillance Research Laboratory
PO Box 1500 SALISBURY SA 5108

13b. Task Sponsor
HQADF

14. Officer/Position responsible for

Security	SOESRL
Downgrading	CEWD
Approval for release	CEWD

15. Secondary Release Statement of this Document

Access additional to the initial distribution list is limited to the Defence Organisation of Australia, US and UK. Others MUST be referred to Chief, Electronic Warfare Division, ESRL.

Any enquiries outside stated limitations should be referred through DSTIC, Defence Information Services, Department of Defence, Anzac Park West, Canberra, ACT 2600.

16a. Deliberate Announcement

May be announced to the Defence Organisation of Australia, US and UK.

16b. Casual Announcement (for citation in other documents)

[√] No Limitation [ ] Ref. by Author, Doc No and date only

17. DEFTEST Descriptors
Horn Antennas Antenna Radiation Patterns
Radar Antennas

18. DISCAT Subject Codes
0049A

19. Abstract

This report describes a technique for calculating the input impedance of ideal, infinitely long TEM horn antennas used to radiate ultrawideband signals. A simple potential calculation is used to determine the fields of the TEM mode of the antenna, from which the input impedance is derived. This result is useful for matching TEM horns to the output impedance of the excitation source to avoid undesirable reflected signals.

DEPARTMENT OF DEFENCE
DEFENCE SCIENCE & TECHNOLOGY ORGANISATION
DSTO

SCIENCE CORPORATE MANAGEMENT BRANCH
DSTO SALISBURY RESEARCH LIBRARY-REPORTS DISTRIBUTION
PO BOX 1500 SALISBURY SA 5108

Reference: R9607/7/9 Pt4 Folio No49
Contact: Natalie Mahlknecht
E-mail: Natalie.Mahlknecht@dsto.defence.gov.au

Telephone: (08) 8259 6255
Facsimile: (08) 8259 6803

18th May 2001

To All Copyholders
cc: To the Team Leader of Records & Archives

Notification of Downgrading/ Delimiting of DSTO Report

Please note that the Release Authority has authorised the downgrading/ delimiting of the report detailed here:

DSTO NUMBER	**DSTO-TR-0187**
AR NUMBER	**AR-009-307**
FILE NUMBER	**UNKNOWN**
PREVIOUS Classification	**WAS:- LIMITED DOD**
REVISED Classification and Release Limitation	**UNCLASSIFIED** **Public Release**

Please amend your records and make changes to your copy of the report itself to reflect the new classification/ release limitation.

Mrs. Natalie Mahlknecht
Reports Distribution Officer
DSTO Research Library, Salisbury